Proposal and Fabrication of Negative-Type Refractive Index Distribution Polymer Optical Fiber

Kenji Tsukada, Yumi Nakagawa, Kouichi Asakura, Eisuke Nihei

Abstract-In this paper, we propose a new type of graded index polymer optical fiber (GI-POF). Most of reported fibers have a convex-type refractive index distribution, where the refractive index is highest at the central axis and gradually decreases as it approaches the cladding region. The fiber presented in this research has a special refractive index distribution that is rarely found in any of the reported polymer optical fibers. We call its distribution "negative refractive index distribution" where the refractive index is lowest around the central axis and highest at the core-cladding boundary.

In this study, we first determined the transmission bandwidth property of the proposed fiber by ray trace simulation. It became clear that with an optimal refractive index distribution, these fibers could have the same transmission bandwidth as conventional refractive index distribution (convex) type fibers.

Furthermore, we were able to show that the proposed fibers could realize easier connecting/branching than conventional fibers because its light intensity becomes highest near the core-cladding boundary. This is verified by simulation of optical branching. These fibers have potential for practical applications such as in high-sensitivity sensors. In addition, when negative refractive index distribution type polymer optical fiber is uniformly excited at incident surface, it is likely that bending loss will not occur because more of the lower-order modes are excited than the higher-order modes.

In this study, we succeeded in actual fabrication of negative refractive index distribution type polymer optical fibers. This fiber is fabricated by two independent means, namely, multi-step interfacial gel polymerization technique and UV-assisted frontal polymerization technique. We measured its refractive index distribution and how much its transmission pulse widened. When pulsed light with full width at half maximum of 140 ps was transmitted for 4.7 m, the pulse widened to 142 ps. This verifies that its band property is sufficient for practical use in short-distance transmission.

Index Terms— polymer optical fiber, negative, refractive index profile, frontal polymerization, branching, UV assist

I. INTRODUCTION

The information network is steadily growing and expanding everywhere in today's world. Over the past few years, an increasing number of people have gained access to the internet and consume bandwidth through activities such as watching on-demand video clips online. The bandwidth of metallic cable network (ADSL network) is not large enough to support such heavy transmission. To meet these high demands in regular households, optical fibers have been introduced as a medium for external transmission. However, they are rarely used within the house, most likely because branching and connecting optical fibers is not an easy task.

The polymer optical fiber (POF) has gathered commercial attention for its easy-to-connect large core diameter and high impact resistance. Graded index type POF (GI-POF) is especially noted for its large bandwidth and has been put to practical use in recent years [1], [2]. Light branching is essential to the formation of network and the optical fiber coupler becomes a factor for high cost to set. If light is branched by contacting fibers, the optical coupler become unnecessary and the physical on-off control of branching should be available. However, contact branching is difficult because transmitted light concentrates at the center of GI-POF

In this study, we propose a particular type of GI-POF that can easily be connected and branched referred to as "negative-type GI-POF (N-GI-POF)." While a conventional GI-POF has a convex-lens-like property, with its refractive index being highest at the central axis (refer to Fig. 1 (a)), N-GI-POF has a refractive index distribution where it is lowest at the central axis and highest at the core-cladding boundary (refer to Fig. 1 (b)). Note that its distribution differs from concave type lens.
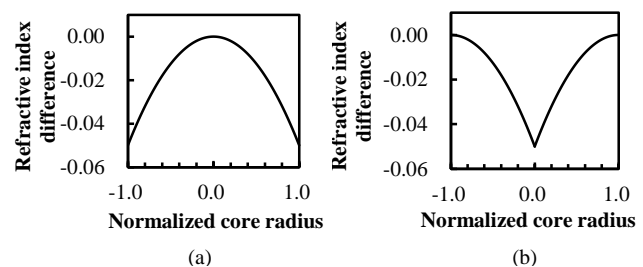
Fig. 1 A conceptual scheme of the refractive index distribution
(a) GI-POF
(b) N-GI-POF.

Light transmitted through N-GI-POF concentrates around the core-cladding boundary. Thus, light can be easily cracked by removing the cladding layer. In other words, the fiber does not need to be cut and re-connected for branching. Simply attaching another N-GI-POF can allow the light to either branch or couple. Furthermore, it is possible to use an external optical amplifier using evanescent wave [3].

In this study, we also assess its bandwidth and contiguous

Kenji Tsukada, Department of Applied Physics and Physico-Informatics, Keio University, Yokohama, Japan,

Yumi Nakagawa, Department of Applied Physics and Physico-Informatics, Keio University, Yokohama, Japan.

Kouichi Asakura, Department of Applied Chemistry, Keio University, Yokohama, Japan.

Eisuke Nihei, Department of Applied Physics and Physico-Informatics, Keio University, Yokohama, Japan.

branching properties estimated by simulation from modal dispersion. Moreover, we actually fabricate N-GI-POF with two methods independently. The first is multi-step interfacial gel polymerization technique. The second is UV-assisted frontal polymerization technique (UVAFP), which is the technique we devised. We also measure its actual bandwidth and refractive index distributions.

II. SIMULATION

A. Ideal negative-type refractive index distribution

The bandwidth of GI-POF is greatly affected by its refractive index distribution. For conventional GI-POF, it has been reported that bandwidth is largest when the refractive index profile is designed to have the smallest modal dispersion [4], [5]. Similarly, we propose that an ideal N-GI-POF is a fiber with a distribution profile that has the smallest modal dispersion. In the presented research, we design the refractive index distribution so that it has the smallest modal dispersion in the meridional direction as shown in Eq. 1.

$$n(r) = \frac{n_0}{\cosh\{\alpha(1-r)\}} = n_0 \operatorname{sech}\{\alpha(1-r)\} \tag{1}$$

Here, α is arbitrary constant and r is normalized radius. The refractive index distribution denoted by Eq. 1 is shown in Fig. 1 (b).

B. Bandwidth calculation

Although there are several methods reported for determining bandwidth from refractive index distribution [6]-[8], there is none for negative-type refractive index distribution with reflection taken into account. Hence, we devised our own calculation method. First, the overall optical path length is calculated by numerical integration of the light ray equation. From this, we derive arrival time of the light ray to a fixed position. We then calculate the impulse response, taking into account of the incident radiation predicted from the radius. Bandwidth is determined by Fourier transformation of the calculated impulse response. Here, it is assumed that incident light ray enters uniformly, and only light rays that enter perpendicular to the core are regarded as incident radiation. It should also be noted that Goos-Hänchen shift is taken into consideration because reflection always occurs in negative-type refractive index distribution.

It has been reported that the overall optical path length could be easily calculated by numerical integration of the light ray equation [9]. Specifically, the combination of the Composite Trapezoidal Rule and numerical integration by Runge-Kutta method allows faster and more precise calculation of optical path length. In this study, we created a calculation program by C language using GCC compiler and GMP library to ensure precision [10].

As noted above, light transmission within N-GI-POF is always accompanied by reflection. When reflection occurs, a Goos-Hänchen shift occurs. Therefore, in this research, we took into account the Goos-Hänchen shift when deriving the overall light ray path length. The Goos-Hänchen shift length is calculated by the following equations [11].

$$d_\perp = \frac{1}{\pi n_1} \cdot \frac{\mu_{12} \sin\theta_1 \cos\theta_1}{\mu_{12}^2 \cos^2\theta_1 + \sin^2\theta_1 - n_{12}^2} \cdot \frac{\lambda}{\sqrt{\sin^2\theta_1 - n_{12}^2}} \tag{2}$$

$$d_\parallel = \frac{1}{\pi n_1} \cdot \frac{\frac{n_{12}^4}{\mu_{12}^2} \sin\theta_1 \cos\theta_1}{\frac{n_{12}^4}{\mu_{12}^2}\cos^2\theta_1 + \sin^2\theta_1 - n_{12}^2} \cdot \frac{\lambda}{\sqrt{\sin^2\theta_1 - n_{12}^2}} \tag{3}$$

Here $d_\perp$ is the Goos-Hänchen shift length of polarized light perpendicular to the plane of incidence, and $d_\parallel$ is that for polarized light parallel to the plane of incidence. n_1 and n_2 are the refractive indexes of the total internal reflection for the core side and cladding side, respectively, and $n_{12} = \frac{n_2}{n_1}$. μ_1 and μ_2 are the magnetic permeability of total internal reflection for the core side and cladding side, respectively, and $\mu_{12} = \frac{\mu_2}{\mu_1} \cong 1$. θ_1 is the angle at which light reflects (incidence angle), and λ is wavelength of light in a vacuum.

The shift length for circular polarized light is given by the following equation.

$$d = \frac{1}{2}(d_\perp + d_\parallel) \tag{4}$$

C. Simulation of contiguous branching of N-GI-POF

In GI-POF, energies of light quanta will gather at a position where refractive index is the highest [12]. In N-GI-POF, refractive index is highest at the core-cladding boundary, so transmitted light rays gather at this position. Thus, we think that light can be easily taken out by simply removing the cladding layer of the fiber. In this research, we verified whether it is possible to branch light by attaching another N-GI-POF to one that already has its cladding layer removed.

III. FABRICATION OF N-GI-POF BY MULTI-STEP INTERFACIAL GEL POLYMERIZATION TECHNIQUE

A. Fabrication of N-GI-POF preform rod

In this research, a preform rod with a negative refractive index distribution and a large diameter is first fabricated. This is then turned into a N-GI-POF by heat drawing of the preform rod.

Multi-step interfacial gel polymerization technique is used for fabricating the preform rod. Unlike simple interfacial gel polymerization where fabrication is performed once, this technique requires interfacial gel polymerization to be performed in many ring layers, gradually forming the rod from the peripheral region toward the central axis. Refer to Fig. 2 for a schematic representation of the technique. The figure shows the polymerization from the first layer (a) to the third layer (c).

This method allows more control over the refractive index profile. By increasing the number of times (steps) that polymerization is performed, the refractive index profile becomes closer to the target design. For this study, polymerization is performed for 7 layers, including the cladding layer, to fabricate the designated refractive index profile.
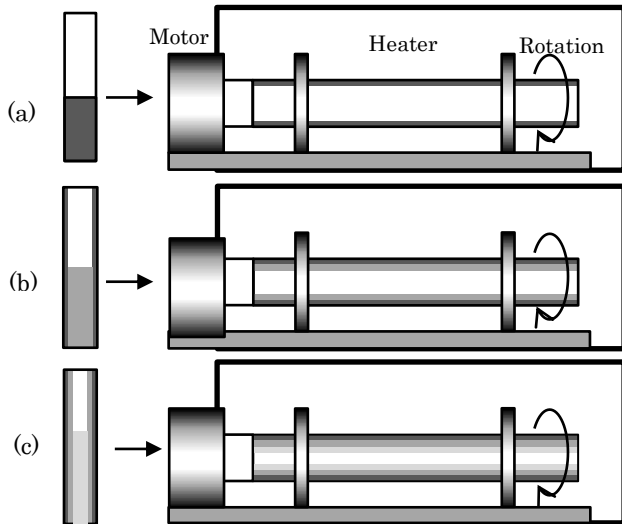
Fig. 2 A schematic representation of multi-step interfacial gel polymerization technique
(a) The first layer
(b) The second layer
(c) The third layer

B. Materials

Methyl methacrylate (MMA; Mitsubishi Rayon Co., Ltd., Tokyo, Japan) is used as the monomer. Benzoyl peroxide (BPO; Nacalai Tesque, Inc., Kyoto, Japan) is used as an initiator and methyl laurate (ML; Wako Pure Chemical Industries) is used as low molecular dopant. n-butyl mercaptan (nBM; Wako Pure Chemical Industries, Tokyo) is used as a chain transfer agent. The monomer is purified by distillation at reduced pressure before use. The function and properties of each material are summarized in Table 1.

Table 1 Materials used for multi-step interfacial gel polymerization technique and their physical properties.

Material	Refractive index	Density (g/cm^3)	Function
Methyl methacrylate (MMA)	1.492 (polymer)	0.943 (monomer) 1.23 (polymer)	Monomer
Benzoyl peroxide (BPO)	-	-	Initiator
Methyl laurate (ML)	1.432	0.87	Dopant
n-butyl mercaptan (nBM)	-	-	Chain transfer agent

A polymerization mixture of monomer and low molecular dopant is prepared for each layer. Table 2 shows the prepared mixture ratio of MMA and methyl laurate of each layer. For all layers, the concentration of BPO and nBM is 0.5 wt % and 0.15 wt % to MMA, respectively.

Extra care is taken so that each layer is polymerized at the same thickness. This is ensured by controlling the quantity of the solution mixture. For this experiment, mixture solutions

are prepared so that each layer will be 1 mm in thickness when polymerized. The outermost layer corresponds to the cladding layer. Hence, its mixture is prepared so that it will have the same refractive index as the central part of the core.

A cylindrical glass with an internal diameter of 14 mm is used as the polymerization container. The prepared solution for the outermost layer is first poured into the container and placed horizontally on a rotating device. It is then polymerized while the container is rotated at 2640 rpm. Polymerization time is set to a time that allows the refractive index distribution to gradually form. The procedure is repeated for five more layers. The last layer (the central region of the rod) is polymerized by setting the container perpendicular and heating it from the lower end.

Table 2 The prepared mixture ratio of MMA and ML for each layer

Layer	ML：MMA
cladding layer	4.0:96.0
1	0.0:100.0
2	0.25:99.75
3	0.5:99.5
4	1.0:99.0
5	2.0:98.0
6 (center)	4.0:96.0

After polymerization, heat treatment is performed at 95 °C for approximately 24 h to finish fabrication of the N-GI-POF preform rod. This preform rod is defined as preform rod A.

C. Fabrication of N-GI-POF

N-GI-POF is fabricated by inserting the preform rod at a fixed speed of V1 into a furnace set to about 250 °C. At the same time, it is pulled out of the furnace at a fixed speed of V2 so that the rod can be heat-drawn into the fiber.

IV. FABRICATION OF N-GI-POF BY UV ASSISTED FRONTAL POLYMERIZATION TECHNIQUE

A. Theory of UVAFP

We devised UVAFP to fabricate N-GI-POF preform rod. UVAFP is an application method of a spontaneous frontal polymerization technique [13], [14] and allows more precise control of the refractive index distribution by irradiating UV light at a partial region of the polymerization container. The procedure of UVAFP is divided into three steps, namely, pre-polymerization, irradiation of UV light and finishing polymerization. Fig. 3 shows the schematic of UVAFP. When the partial region of the monomer is irradiated with UV light, the gel-monomer interface (front) appears. As the polymerization proceeds, the front moves towards the monomer region by Trommsdorff-Norrish effect [15]. Refractive index gradient is formed when the moving front extrudes low molecular dopant. At this point, when the shape of UV light is thin and parallel as laser, axial graded-index

distribution forms.
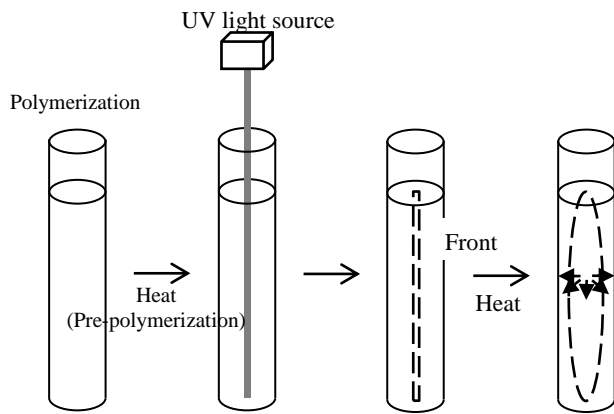
Fig. 3 Schematic of UVAFP.

In spontaneous frontal polymerization technique, POF could not be fabricated, because front is generated by the heat accumulation and that needs cross-linking agent. On the other hand, in UVAFP, front is generated by UV light. Thus cross-linking agent is unnecessary and the heat drawing of preform rod is available.

Moreover the front configuration could be controlled. The preform rod with a particular type of refractive index distribution like N-GI distribution is fabricated. It will be possible to fabricate an axis-shifted GI waveguide that is able to focus through bending waveguide [16] by displacing the UV irradiation point from the center, or to fabricate multi-core GI-POF using plural light source.

Refractive index distribution formed by this technique depends on various experiment conditions for example the UV irradiation time range or the temperature of the polymerization in each step mentioned above. However once the appropriate condition is found for the objective distribution, the preform rod is fabricated reproducibly with easy manipulation. N-GI-POF preform rod is obtained by setting proper experiment conditions. The conventional GI-POF preform rod can be also fabricated by changing conditions.

B. Fabrication of N-GI-POF preform rod

Diphenyl sulfide (refractive index = 1.633) is used as a low molecular dopant. 2-Hydroxy-2-methylpropiophenone is used as a photo polymerization initiator. Both reagents were purchased from TOKYO CHEMICAL INDUSTRY Co., Ltd, Tokyo, Japan.

Monomer solution is prepared with MMA, DPS, nBM, BPO, and HMP. The concentration of DPS, nBM, BPO, and HMP is 15.0 wt %, 0.08 wt %, 0.3 wt % and 0.04 wt % to MMA, respectively. Mixture is given nitrogen substitution for 1 min and degassed by ultrasonic wave for 20 min before being injected into the glass tube. The inner diameter of the glass tube is 14.5 mm, and the height of the solution from the bottom is 150 mm. The polymerization container is put into an oil bath at 85 °C for 3 h and 40 min. As a UV laser light source, UV-F-355 (Sun Instruments, wave length = 355 nm, 5.15 mW) is used. UV irradiation is performed in the air at room temperature. UV light is irradiated from top of the polymerization container as shown in Fig. 3 for approximately 18 min. We took extra care to point the laser at the center of monomer surface. After the irradiation, the container is placed in air at 82 °C for approximately 48 h for

heat treatment. The glass tube is removed with the produced preform rod. Then an additional heat treatment is conducted under the air condition at 90 °C for approximately 48 h. This preform rod is defined as preform rod B.

V. MEASUREMENTS

A. Refractive index distribution of the fabricated N-GI-POF preform rod

Refractive index distribution of the fabricated preform rods are measured by a non-destructive method which uses a street type laser light [17]. The preform rod must be set in a bath of matching oil that has the same refractive index as the peripheral region (cladding layer). For this experiment, the cladding layer of the fabricated preform rod had a refractive index of 1.485. Therefore, the matching oil with almost the same refractive index was used for the measurement.

Refractive index distribution of preform rod B was measured by the same method. The refractive index of immersion oil was 1.517.

B. Bandwidth of the fabricated N-GI-POF

The bandwidth of the fabricated N-GI-POF is derived from how much the pulse of the transmitted light broadened. A pulse laser diode (wavelength = 656.5 nm) is used as the light source, and an optical sampling oscilloscope OOS-01 (Hamamatsu photonics K.K.) is used as the detector.

VI. RESULTS OF SIMULATION

A. Bandwidth prediction by approximation of refractive-index distribution

An ideal refractive index distribution that gives N-GI-POF a large bandwidth is denoted by Eq. (1) containing sech function. However, the sech function cannot be directly calculated in a GMP library. Therefore, an approximate expression of the polynomial of sech function is used. Eq. (1) is transformed to an approximate equation as shown in Eq. (5).

$$n(x) = n_0 \left(1 - \frac{\{\alpha(1-x)\}^2}{2} + \frac{5\{\alpha(1-x)\}^4}{24} - \frac{61\{\alpha(1-x)\}^6}{720} \cdots \right) \quad (5)$$

In this research, the bandwidth is calculated from Fourier transformation of impulse responses. The 2nd and 3rd term of the approximate expressions above are used for calculating impulse responses. For comparison, we not only calculated bandwidth for N-GI-POF, but also a positive GI-POF by the same given method. Moreover, we also calculated bandwidths with Goos-Hänchen shift. The calculated results are shown in Table 3 and 4.

Table 3 Bandwidth estimation of positive and negative GI-POF without Goos-Hänchen shift (2ⁿᵈ and 3ʳᵈ term approximation)

Approximation	Type	
	Positive	Negative
Two-terms	67 Gbit/s	540 Gbit/s
Three-terms	8.5 Tbit/s	6.0 Tbit/s

Table 4 Bandwidth estimation of positive and negative GI-POF with Goos-Hänchen shift (2ⁿᵈ and 3ʳᵈ term approximation)

Approximation	Negative Type
Two-terms	680 Gbit/s
Three-terms	6.0 Tbit/s

As shown in Table 3, the estimated bandwidths of both positive and negative GI-POF without Goos-Hänchen shift are larger when approximated to a higher order.

When using 2ⁿᵈ term approximation, the bandwidth of N-GI-POF is larger than positive GI-POF. This is probably because N-GI-POF transmits more lower-order mode lights than positive GI-POF. When using 3ʳᵈ term approximation, the estimated bandwidths of both positive and negative GI-POF have almost the same bandwidth as fibers with modal dispersion. These values are much greater than bandwidth limit of a PMMA-based fiber with modal dispersion [8]. This indicates that N-GI-POF has sufficient bandwidth to be used as an optical transmission medium.

The calculation results of the bandwidth of N-GI-POF with and without Goos-Hänchen shift are almost equal. This indicates that Goos-Hänchen shift hardly has any effect on the bandwidth of N-GI-POF. Fig. 4 shows the Goos-Hänchen shift length when light is transmitted through a 100 m of N-GI-POF. The vertical axis Goos-Hänchen shift length, and the horizontal axis represents the light incident position from the center axis (incidence radius) of the N-GI-POF. The shift length is greatest near the central axis. Yet it is only about 0.3 mm, which is small enough to be ignored when calculating overall optical path length.
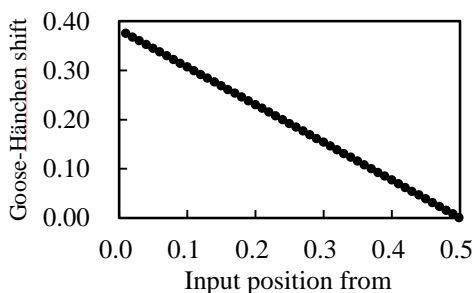
Fig. 4 Relationship between incidence radius and total Goos-Hänchen shift length (fiber length = 100 m).

B. Simulation of contiguous branching

Fig. 5 shows the calculation result of ray trajectory at contiguous branching of N-GI-POF (Fig. 5 (a)) and refractive index distribution (Fig. 5 (b)) at the contact point of the fibers. In this case, it is presumed that fiber 1 and 2 have same properties.

Light transmits as it continuously reflects at the cladding layer. When two N-GI-POFs touch each other, the contact point has a refractive index distribution similar to that of the positive GI-POF. This profile will allow light to transfer to the attached fiber. However, if contact length is beyond pitch length, the light may return to the original fiber. Therefore, extra care is required when contiguously branching.
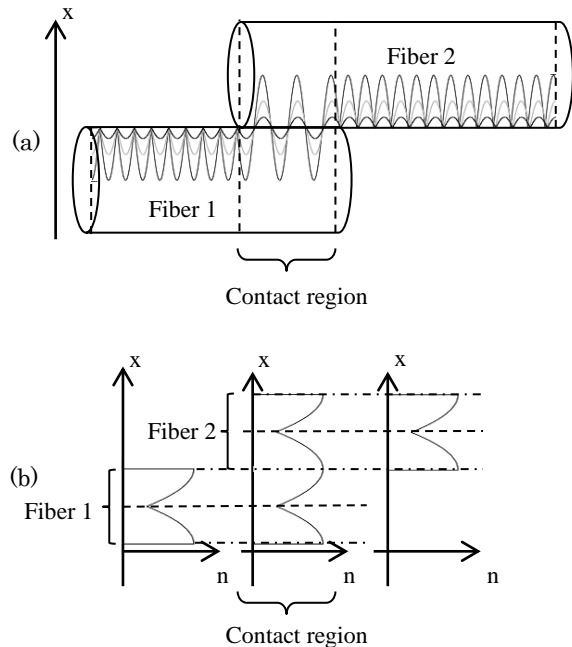
Fig. 5 A conceptual scheme of contiguous branching of fibers
(a) Ray trajectory at the contact N-GI-POF
(b) Refractive index distribution at the contact point

VII. RESULTS OF FABRICATION

A. Refractive index distribution

Fig. 6 shows the measured refractive index distribution of the preform rod A. The vertical axis is the normalized radius of the preform rod and the horizontal axis is the refractive index.
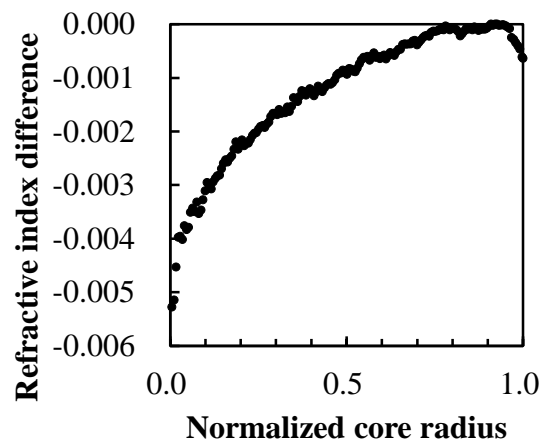
Fig. 6 Refractive index distribution of the fabricated N-GI-POF preform rod (preform rod A)

The refractive index distribution of fabricated fiber heat-drawn from the preform rod has almost the same refractive index distribution of preform rod [18]. Likewise, N-GI-POF fabricated in this research will have the same refractive index distribution as the preform rod.

Although the refractive-index distribution of N-GI-POF fabricated for this research is not an ideal refractive index distribution denoted by Eq. (1), it could be realized by more precise control during polymerization.

The refractive index distribution of preform rod B is shown in Fig. 7. Although the shape is not the negative distribution near the center, in such a region the power of light is low. Therefore this is considered as N-GI distribution as a whole. The distribution of preform rod B has a large refractive index difference. That is not because of UVAFP, but because of the concentration of low molecular dopant and the refractive index difference between the dopant and the polymer. The curve shown in Fig. 7 is smooth because the refractive index distribution is formed in one step with UVAFP.

In the experiment, the front generated by UV laser is uniform in shape along the optical axis, because the concentration of photo polymerization initiator is very small. The power of UV light is relatively uniform from top to bottom of the polymerization container. Therefore, refractive index distribution of the obtained preform rod is also uniform along the optical axis.
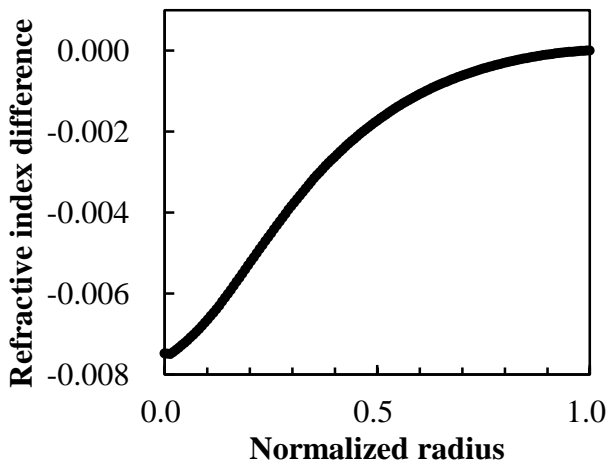
Fig. 7 Refractive index distribution of the preform rod B

B. Bandwidth

As suggested in a previous report [19], the bandwidth of experimentally produced N-GI-POF was calculated from the full width at half maximum (FWHM) of the input and output signals using an optical sampling oscilloscope. Estimation is calculated as follows:

$$\text{Bandwidth} = \frac{0.44}{\sqrt{\tau_2{}^2 - \tau_1{}^2}} L \qquad (6)$$

Here L is the length of fiber, and τ_1 and τ_2 are the FWHM of the input and output signals, respectively. With respect to N-GI-POF fabricated with multi-step interfacial gel polymerization technique, FWHM of the output signal at 5.7 m and 1 m are 142 and 140 ps, respectively. Applying these results to Eq. (6), the bandwidth of N-GI-POF is 870 Mbit/s at 100 m. Compared with GI-POF previously reported [20], it is very small. Since all pulses are presumed to be Gaussian, it

is necessary to use Fourier transformation to determine a more accurate bandwidth. In the same way, the bandwidth of N-GI-POF fabricated with UVAFP is 500 Mbit/s at 100 m.

REFERENCES

[1] M. Asai, Y. Inuzuka, K. Koike, S. Takahashi, and Y. Koike, "High-bandwidth graded-index plastic optical fiber with low-attenuation, high-bending ability, and high-thermal stability for home-networks," *J. Lightwave Technol.* vol. 29, 2011, pp. 1620–1626.

[2] C. H. Chang, W. Y. Lin, H. H. Lu, C. Y. Chen, P. Y. Wu, and Y. P. Lin, "An integrated long-reach PON and GI-POF in-house network architecture for hybrid CATV/OFDM signals transmission," *J. Lightwave Technol.* vol. 30, 2012, pp. 3247–3251.

[3] T. Hirai and E. Nihei, "Fabrication of defocus graded-index optical waveguide for evanescent wave optical amplifier," *Opt. Rev.* vol. 21, 2014, pp. 110–116.

[4] S. Kawakami and J. Nishizawa, "Kinetics of an optical wave packet in a lens-like medium," *J. Appl. Phys.* vol. 38, 1967, pp. 4807–4811.

[5] S. Kawakami and J. Nishizawa, "An optical waveguide with the optimum distribution of the refractive index with reference to waveform distortion," *Microwav. Theory Techn., IEEE Trans.* vol. 16, 1968, pp. 814–818.

[6] R. Olshansky and D. B. Keck, "Pulse broadening in graded-index optical fibers," *Appl. Opt.* vol. 15, 1976, pp. 483–491.

[7] T. Ishigure, E. Nihei, and Y. Koike, "Optimization of the refractive-index distribution of high-bandwidth GI polymer optical fiber based on both modal and material dispersions," *Polym. J.* vol. 28,1996, pp. 272–275.

[8] T. Ishigure, E. Nihei, and Y. Koike, "Optimum refractive-index profile of the graded-index polymer optical fiber, toward gigabit data links," *Appl. Opt.* vol. 35, 1996, pp. 2048–2053.

[9] A. Sharma, "Computing optical-path length in gradient-index media - a fast and accurate method," *Appl. Opt.* vol. 24, 1985, pp. 4367–4370.

[10] "The GNU Multiple Precision Arithmetic Library", Available: http://gmplib.org/ accessed on November 2, 2016.

[11] R. H. Renard, "Total reflection: A new evaluation of the Goos–Hänchen shift," J. Opt. Soc. America vol. 54, 1964, pp. 1190–1197.

[12] F. M. E. Sladen, D. N. Payne, and M. J. Adams, "Determination of optical fiber refractive-index profiles by a near-field scanning technique," *Appl. Phys. Lett.* vol. 28, 1976, pp. 255–258.

[13] K. Asakura, E. Nihei, H. Harasawa, A. Ikumo, and S. Osanai, "Spontaneous frontal polymerization: Propagating front spontaneously generated by locally autoaccelerated free-radical polymerization," in *Nonlinear Dynamics in Polymeric Systems*, J. A. Pojman and Q. TranCongMiyata, Eds., American Chemical Society,Washington, DC, 2004, pp. 135–146.

[14] E. Nihei, J. Oomoto, S. Kimura, and K. Asakura, "Preparation and characterization of organic-inorganic microcomposite cylindrical GRIN lens," *Polym. J.* vol. 42, 2010, pp. 941–946.

[15] B. Oshaughnessy and J. Yu, "Autoacceleration in free-radical polymerization .1. conversion," *Macromol.* vol. 27, 1994, pp. 5067–5078.

[16] A. Ghatak, E. Sharma, and J. Kompella, "Exact ray paths in bent wave-guides," *Appl. Opt.* vol. 27, 1988, pp. 3180–3184.

[17] E. Nihei and S. Shimizu, "Determination of the refractive index profile of polymer optical fiber preform by the transverse ray tracing method," *Opt. Commun.* vol. 275, 2007, pp. 14–21.

[18] Y. Koike, "High-bandwidth graded-index polymer optical fibre," Polymer 32, 1991, pp. 1737-1745.

[19] C. Koeppen, R. F. Shi, W. D. Chen, and A. F. Garito, "Properties of plastic optical fibers," J. Opt. Soc. Am. B-Opt. Phys. 15, 1998, pp. 727-739.

[20] B.-G. Shin, J.-H. Park, and J.-J. Kim, "Low-loss, high-bandwidth graded-index plastic optical fiber fabricated by the centrifugal deposition method," *Appl. Phys. Lett.* vol. 82, 2003, pp. 4645–4647.